

# 1 Electroactive biofilters outperform inert biofilters for treating surfactant-polluted wastewater 2 by means of selecting a low-growth yield microbial community

3 Eduardo Noriega Primo <sup>1,2</sup>, María Isabel López Heras<sup>3</sup> and \*Abraham Esteve-Núñez <sup>1,3\*</sup>

4

5 <sup>1</sup>Universidad de Alcalá, Department of Analytical Chemistry, Physical Chemistry and Chemical Engineering, Ctra. Madrid-Barcelona KM 33.600, 28871  
6 Alcalá de Henares, Madrid, Spain.

7 <sup>2</sup>Metfilter S.L. Autovía A49, Sevilla-Huelva, Km. 28, 41820 Carrión de los Céspedes, Sevilla, Spain

8 <sup>3</sup>MDEA Water Institute, Av. Punto Com, 2, 28805 Alcalá de Henares, Madrid, Spain

9 \* abraham.esteve@uah.es

10

11 Corresponding author: Dr. Abraham Esteve-Núñez

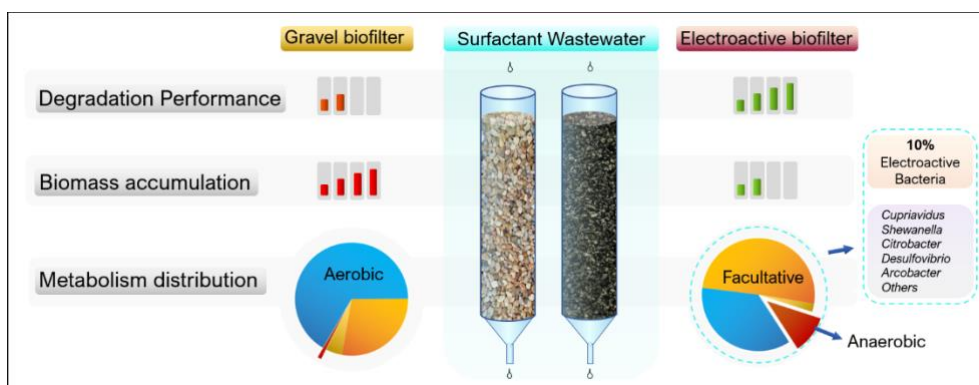
12 Associate Professor, Associate Researcher of IMDEA WATER, Bioe Group,

13 Chemical Engineering Department, University of Alcalá, Madrid, Spain. +34-918854950

14

Keywords:

Surfactants  
Biodegradation  
Biomass accumulation  
Electroactive  
microorganisms  
Wastewater treatment



15

16

## 17 Abstract

18

19 Electrobioremediation is one of the most innovative disciplines for treating organic pollutants and it is  
20 based on the ability of electroactive bacteria to exchange electrons with electroconductive materials.  
21 Electroactive biofilters have been demonstrated to be efficient for treating urban wastewater with a  
22 low footprint; however, their application can be expanded for treating industrial wastewater containing  
23 significant concentrations (2.4 %<sub>vol</sub>) of commercial surfactants (containing lauryl sulfate, lauryl ether  
24 sulfate, cocamydopropyl betaine, and dodecylbenzene sulfonate, among others). Our electroactive  
25 biofilter outperformed a conventional inert biofilter made of gravel for all tested conditions, reaching  
26 removal rates as high as 4.5 kg COD/m<sup>3</sup><sub>bed</sub>·day and withstood Organic Loading Rates as high as 9 Kg  
27 COD/m<sup>3</sup>·d without significantly affecting removal efficiency. The biomass accumulation reduced  
28 available bed volume in the electroactive biofilter just by 39%, while the gravel biofilter decreased by  
29 80%. Regarding microbial communities, anaerobic and electroactive bacteria represented a substantial  
30 proportion of the total population in the electroactive biofilter. *Pseudomonas* was the dominant genus,  
31 while *Cupriavidus*, *Shewanella*, *Citrobacter*, *Desulfovibrio*, and *Arcobacter* were potential

32 electroactive strains found in relevant proportions. The microbial community's composition might be  
33 the key to understanding how high removal rates can coexist with limited biomass production, making  
34 electroactive biofilters a promising strategy to overcome classical biofilter limitations.

35

## 36 **1 Introduction**

37 Surfactant pollution in aquatic environments has been of concern since its spread as a household  
38 commodity. In the past century, the authorities detected that the early market-available surfactants  
39 generated significant foaming problems in the sewage and wastewater treatment plants and were found  
40 to have limited biodegradability. Common detergent products mainly combine anionic and nonionic  
41 surfactants to enhance their properties. Anionics accounted for around 70% of global surfactant  
42 production (Liwarska-Bizukojc et al., 2005). However, they are being partially replaced in  
43 formulations by amphoteric surfactants, which are more stable, less toxic and irritating, and more  
44 biodegradable (Sarkar et al., 2021).

45 Surfactants are indeed abundant in urban wastewater and apart from the possible direct discharges  
46 without treatment, the main route for surfactants to reach the environment is wastewater treatment  
47 plants (WWTP) operating under distress, episodes of sludge reuse, or discharge in landfills. Surfactants  
48 might cause disturbances in primary wastewater treatment, but in the secondary treatment, over 90%  
49 of the most common surfactants are removed (Arora et al., 2022; Camacho-Muñoz et al., 2014;  
50 Ivanković & Hrenović, 2010). Surfactant concentrations that generate foam significantly disturb the  
51 operation of WWTPs, leading to poor-quality effluents (Berna et al., 1991).

52 The decreased surfactant concentration observed in WWTP can be attributed to sorption on sludge and  
53 biodegradation (Schinkel et al., 2022). Surfactants tend to attach to anaerobic sludge particles where  
54 biodegradation may occur, although those seem more effectively degraded by aerobic biofilm-forming  
55 organisms (Ying, 2006). Most surfactants in household detergents are biodegradable under aerobic  
56 conditions, but only a few are degradable when oxygen is limited (Merrettig-Bruns & Jelen, 2009).  
57 This oxygen dependence was confirmed when linear alkyl-benzene sulfonate's (LAS) presence in  
58 anaerobic sludge was between 1 to 2 orders of magnitude higher than in aerobically treated sludge as  
59 a fraction of dry mass (Jensen, 1999).

60 Biodegradation pathways for the most common surfactants have already been determined. Sodium  
61 dodecyl-benzene sulfonate (SDBS) breakdown involves the cleaving and degrading of the alkyl chain,  
62 the benzene ring, and a sulfonate ring that eventually transforms into  $\text{SO}_4^{2-}$ . The degradation of the

63 alkyl chain starts with the  $\omega$ -oxidation of the terminal methyl group. As for de-sulfonation, three  
64 mechanisms have been proposed: hydroxylative de-sulfonation, monooxygenase catalysis, and  
65 reductive de-sulfonation. After that, the sulfite can be oxidized to sulfate. Eventually, these cleavages  
66 result in phenylacetic or benzoic acids. Finally, these acids can be transformed into fumaric and  
67 acetoacetic acids and converted to catechol (Scott & Jones, 2000). For sodium lauryl ether sulfonate  
68 (SLES), the first step for degradation can be ether cleavage or ester cleavage, releasing intermediates  
69 further decomposed by  $\beta$ -oxidation until mineralization (Paulo et al., 2017).

70 Over the last decades, several studies have tried to provide solutions for the treatment of surfactant  
71 wastewater under different disciplines: electrochemical treatment (Panizza et al., 2005), Fenton  
72 oxidation (X. J. Wang et al., 2008), adsorption (Kim et al., 2019), and coagulation combined with  
73 biological treatment (Aloui et al., 2009), among others. Regarding more sustainable and natural  
74 solutions, artificial/constructed wetlands have been proposed to treat surfactant-containing wastewater  
75 (Justin et al., 2009; Šíma & Holcová, 2011).

76 In this sustainability scenario, a recent strategy, named electrobioremediation, bridges the gap between  
77 high-efficiency treatments and passive bio-based treatments under a natural and sustainable scheme  
78 (X. Wang et al., 2020). In fact, electrobioremediation is based on the singular capabilities of  
79 electroactive microorganisms to couple the oxidation of organic matter with the respiration of  
80 electroconductive materials (electrodes). This coupling minimizes the respiration bottleneck in  
81 anaerobic environments, where the availability of the terminal electron acceptor (TEA) like  $O_2$  is  
82 limited. This disruptive discovery (Bond & Lovley, 2003) led to the development and rapid expansion  
83 of microbial electrochemistry, which continues to show promising applications in environmental  
84 protection and recovery and, more specifically, in water treatment strategies.

85 Recently, a study was carried out for the simultaneous energy recovery and treatment of real carwash  
86 wastewater (Radeef & Ismail, 2021). Surfactants have also been studied as additives in  
87 bioelectrochemical reactors like Microbial Fuel Cells, where their presence enhanced the  
88 bioavailability of hydrophobic substances (Hwang et al., 2019), improved biofilm formation by  
89 interacting with the surface of the electrode (Zhang et al., 2017), and seemed to produce a synergistic  
90 effect with electron shuttles (Pham et al., 2008).

91 Originally the concept electroactive biofilter resulted from the process integration of microbial  
92 electrochemistry into a biofilter-based natural concept as treatment wetlands, where a natural  
93 ecosystem operates in equilibrium to remove organic matter with no energy requirements. Indeed,  
94 replacement of inert bed with electroconductive material enables the connection of differing redox

95 environments and the selection of electroactive microorganisms (EAM). The new configuration  
96 included plants and it was named METland® (Aguirre-Sierra et al., 2016). Indeed, a redox gradient is  
97 formed by creating this electrical connection along the bed, allowing the flow of electrons from the  
98 anaerobic locations towards the oxidative areas (O<sub>2</sub> rich), thus, providing EAM with an unlimited sink  
99 of electrons. Initially these systems were operated under the microbial electrochemical snorkel (MES)  
100 configuration, where the circuit assembly sacrifices current production to enhance catabolic activity  
101 (Aguirre-Sierra et al., 2016). As this open circuit alleviates TEA limitation, pollutant removal is  
102 maximized. METland® originally operated under flooded conditions, and the electron flux was  
103 confirmed and measured using a custom-made electric potential sensor (Peñacoba-Antona et al.,  
104 2022a; Prado et al., 2020, 2022; Ramírez-Vargas et al., 2019). A METland® can also be operated in a  
105 downflow non-flooded mode (Aguirre-Sierra et al., 2020), taking advantage of a passive supply of air,  
106 where the aerobic and anaerobic environments (outer and inner layers of biofilm, respectively)  
107 generate redox gradients at micro-scale in the stratified layers of the biofilm. In fact, biofilms play a  
108 key role in bioelectrochemical processes since higher cellular densities account for more cellular  
109 proximity and contact, increasing electron transfer possibilities (Yang et al., 2012). METland have  
110 been demonstrated at full scale using Life Cycle Assessment as validation tool (Peñacoba-Antona et  
111 al., 2021).

112 This study aims to validate lab-scale electroactive biofilters for treating wastewater containing anionic  
113 and amphoteric surfactants, including operational and performance factors. In spite of the harsh  
114 environment of surfactant-polluted wastewater, the microbial community was characterized to reveal  
115 how high biodegradation rates can coexist with limited biomass production.

116

## 117 **2 Materials & Methods**

### 118 **2.1 Wastewater composition.**

119 Synthetic wastewater was prepared using a salt medium and a mixture of commercial detergent  
120 products. The salt medium composition was: 0.4 g/L of sodium bicarbonate (NaHCO<sub>3</sub>), 0.04 g/L of  
121 ammonium chloride (NH<sub>4</sub>Cl), 0.04 g/L of calcium chloride dihydrate (CaCl<sub>2</sub>·2H<sub>2</sub>O), 0.03 g/L sodium  
122 dihydrogen phosphate (NaH<sub>2</sub>PO<sub>4</sub>), 0.02 g/L potassium nitrate (KNO<sub>3</sub>), 0.02 g/L magnesium chloride  
123 hexahydrate (MgCl<sub>2</sub>·6H<sub>2</sub>O), 0.02 g/L of potassium chloride (KCl) and 0.02 g/L of iron sulphate  
124 heptahydrate (FeSO<sub>4</sub>·7H<sub>2</sub>O) (5% weighting error).

125 The concentration of the detergent mixture was dependent on the experiment, but 2.4% by volume on  
126 water was the concentration typically used (ca.  $5100 \pm 200$  ppm of chemical oxygen demand (COD)).  
127 The proportion of commercial detergent products in the mixture was selected to emulate a hypothetical  
128 composition of a detergent production factory wastewater. This concentration was kept constant for  
129 all experiments: 50% dishwasher soap (Carrefour Expert Lemon dishwasher, Carrefour, France), 20%  
130 laundry detergent (Carrefour Expert Optimal Clean, Carrefour, France), 20% toilet detergent (Eco  
131 Planet Eucalyptus WC detergent, Carrefour, France), and 10% glass cleaning detergent (Carrefour  
132 generic glass cleaner, Carrefour, France). The surfactant components mentioned in the labels are  
133 sodium lauryl ether sulfate (SLES), Cocamidopropyl betaine (CAPB), sodium C14-16 olefin sulfonate,  
134 and methyl alkyl benzene sulfonate (ME-DBS). It also contains alcohol ethoxylated surfactants and  
135 additives such as methylchloroisothiazolinone, methylisothiazolinone, and phenoxyethanol.

136 The real surfactant wastewater was prepared using the same salt medium and dissolving a concentrated  
137 mixture of residual detergents provided by a detergent factory that produces similar detergent products  
138 as those mentioned before.

139 For the experiments with single surfactants, the products used were: sodium lauryl sulfate (SLS),  
140 sodium lauryl ether sulfate (SLES), and Cocamidopropyl betaine (CAPB) (Guinama S.L., Spain);  
141 sodium dodecylbenzene sulphonate (SDBS), Tween 80, and Triton X-100 (Sigma Aldrich, USA).

142

## 143 **2.2 Analytical Methods**

144 COD was determined using a cuvette test from (LCK Hach), digested in an HT200S (Hach Lange,  
145 USA) thermostatic digester, and measured using a DR 3900 spectrophotometer (Hach Lange, USA).  
146 The conductivity was measured with a conductometer GLP 31 (Crison, Spain), and the pH was  
147 measured with the pH-meter Basic 20+ (Crison, Spain). Sulfate was measured using a Metrom  
148 Compact IC model 930 ionic chromatograph.

149 The specific chemical identifications were performed with an Agilent Technologies 1200 HPLC  
150 (Agilent Technologies, USA), coupled to an Agilent Technologies 6230 MS-TOF (Agilent  
151 Technologies, USA), using an Acclaim Surfactant Plus column (150mm x 3mm x3  $\mu$ m) (Thermo  
152 Fisher, USA). The mobile phase was ammonium acetate 0,1M at pH 5 (A) and acetonitrile (B), run at  
153 0.6ml/min, 25 °C, and 5 $\mu$ L sample injection. Further details can be found in supplementary section II  
154 table 7.

155

## 156 2.3 Experiments and Set-ups

### 157 2.3.1 Impact of material nature on biomass formation and hydraulic conductivity

158 A comparative experiment was made using two identical glass reactors consisting of single cylinder  
159 pieces 50 cm long and 6 cm of internal diameter, narrowing down at the bottom to 0.8 cm. Each one  
160 was filled with 0.8L of electroconductive carbonaceous material (METFILTER SL, Spain) or gravel,  
161 with a 6-8 mm granulometry, and inoculated with a microbial consortium available in our research  
162 group. This specific set-up was designed to maximize granule comparability and allow gravity  
163 drainage trials. The same detergent-based synthetic wastewater was continuously fed to both systems  
164 (1.6 L/d), following a sequence i) fresh media for 5 days and ii) 2 days reusing the effluent. Initially,  
165 there was no biomass in the system, and its development was evaluated periodically over 72 days of  
166 operation.

167 Two different experiments were carried out to evaluate the impact of biomass growth on the biofilters'  
168 hydraulic characteristics.

169

#### 170 Residence time distribution using a tracer:

171 Pulse tracer experiments were conducted to determine the residence time distribution using potassium  
172 bromide (KBr) as a tracer. Bromide was selected as a tracer mainly because: i) given its negative  
173 charge, it was expected to behave similarly to anionic surfactants; ii) it has little interaction with  
174 microbial life.

175 A tracer solution was pulsed for 5 minutes, after which the columns were returned to regular operation.  
176 The flow rate and the surfactant content were not altered during this period. Samples were collected  
177 periodically during the experiment, which lasted around 120 minutes.

178 The residence time distribution (RTD) is represented such that only the recovered tracer is considered  
179 the area below the curve, not considering here losses on recovery.

$$180 \int_0^{\infty} E dt = 1$$

181 The residence-time distribution function ( $E(t)$ ) is obtained from the normalization of the concentration  
182 curve, which is determined by the changing effluent tracer concentrations over time.

$$183 E(t) = \frac{C(t)}{\int_0^{\infty} C(t) dt}$$

184 The mean residence ( $t_m$ ) time can be obtained from the dataset mathematically as follows:

185 
$$t_m = \frac{\int_0^{\infty} tE(t)dt}{\int_0^{\infty} E(t)dt} = \int_0^{\infty} tE(t)dt$$

186 Another parameter that aids in the characterization of the curves is the variance or square of the  
187 standard deviation ( $\sigma^2$ ):

188 
$$\sigma^2 = \int_0^{\infty} (t - t_m)^2 E(t)dt$$

189 This descriptive parameter indicates the distribution's breadth (Fogler, 2006).

190

### 191 **Hydraulic conductivity measurements:**

192 The measurement of hydraulic conductivity was based on Darcy's law.  $K_v$  was determined following  
193 a gravity drainage method (Gefell et al., 2019). The method was modified by applying a constant  
194 hydrostatic head of 5 cm of water for comparability between reactors. During the test, the water  
195 flowing out of the biofilter was collected in a graduated vessel, the volume and time were registered.  
196 Then the flow rates were calculated, and the average served for further calculating the  $K_v$ .

197 
$$K_v = \frac{Q}{\left[ \frac{A dh}{dL} \right]}$$

198  $K_v$  is the vertical hydraulic conductivity,  $Q$  is the measured flow rate at the outlet,  $A$  is the outflow  
199 area,  $dh$  is the hydraulic pressure differential (complete water column), and  $dL$  is the column height  
200 occupied by material.

201 For the measurements of available volume and hydraulic conductivity, the columns were slowly  
202 flooded to prevent the trapping of air. Then the water was released, and its volume was measured. The  
203 initial values with no biomass were compared to the final values with biomass growth after 72 days.

204

### 205 **2.3.2 Biofilter operation**

206 The following experiments focused on studying the operation and validation of lab-scale electroactive  
207 biofilters to treat surfactant-polluted water using a specific set-up different from the previous one.

208

209 The electroactive biofilter was filled with carbonaceous electroconductive material (3-7 mm), and the  
210 control biofilter was filled with gravel (3-8 mm). In both cases, 0.8 L of material was used. The biofilter

211 reactor consisted of a glass cylinder (43cm high and a 6cm inner diameter)—a second internal glass  
212 cylinder of 1 cm diameter had 3 mm perforations serving as a passive aerator.

213 The biofilters were operated indoors at  $23\pm 2$  °C under a down-flow mode using a peristaltic pump  
214 (Watson Marlow 323). These biofilters were continuously fed, and the flow rate was adjusted from 0.4  
215 L/d to 1.6 L/d, feeding an amount of  $5200\pm 200$  mg COD/ L.

216 The inoculum was the same for both systems, using urban wastewater and a heterogeneous  
217 electroactive consortium (Metfilter S.L.).

218 The comparative performance was tested under continuous operation. Two experiments were  
219 designed: i) non-steady-state performance at 0.4 L/d during 7-9 days of operation and the sampling for  
220 3 consecutive days; then the reactor was dismantled, bed was flushed with water, and restarted (new  
221 flow rate); ii) For the steady-state condition, a biofilter was monitored at 1 L/d, after reaching stable  
222 COD values at the effluent.

223 Another experiment for evaluating the performance and biodegradability of the surfactant mixture was  
224 carried out under batch by continuously recirculating a fixed volume of wastewater. The batch  
225 experiments were carried out twice, and the results displayed correspond to the last ones. Experiments  
226 with both real and synthetic wastewaters were set for several days in a close circuit recirculation at a  
227 flow rate of 1 L/d and a tank volume of 1L. HPLC-MS analysis of these waters samples was carried  
228 out to provide more precise evidence of molecular degradation and determine the differences in the  
229 composition of the synthetic and real waters.

230

### 231 **2.3.3 Culture vessel experiments with single surfactants:**

232 Six glass culture vessels of 100 ml (Pobel, Spain) were filled with 35 grams of colonized conductive  
233 carbonaceous material. Each surfactant was dissolved in the freshwater medium to achieve a COD  
234 value of  $3500\pm 200$  ppm. Biodegradation tests were performed by adding 20ml of surfactant solution  
235 (a solution for each surfactant), and all of them were kept in an orbital incubator at 30 °C and 120 rpm.

236 The medium was replaced with new medium every week during the acclimation period. COD and  
237 HPLC-MS analysis were made on the 6<sup>th</sup> and 10<sup>th</sup> cycle.

238 Abiotic controls with fresh and autoclaved material were tested to evaluate adsorption. Planktonic  
239 controls, without bed material, were maintained for three surfactants to compare the effects of  
240 inoculated material for biodegradation.



241 The Triton X-100 was selected for solvent extraction, given that it had the lowest limit of quantification  
242 in the HPLC-MS. For the adsorption evaluation, 2 grams of sample material were taken from the  
243 culture vessel subject to four runs. Another sample of 2 grams from a replicate was exposed to the  
244 surfactant once. After two-stage organic extraction (methanol and acetonitrile) and resuspension in  
245 deionized water, samples were injected into the HPLC-MS.

246

#### 247 **2.3.4 Microbial community evaluation**

248 Three independent colonized granules from biofilters (*ca.* 4 cm bed depth) were selected and stored at  
249 -80 °C. DNA extraction, PCR amplification, and high-throughput sequencing were performed by an  
250 external service for genomic analysis (Institute of Biotechnology and Biomedicine, UAB, Barcelona).

251 The V3-V4 region of the 16S bacterial gene was amplified by a polymerase chain reaction (PCR) with  
252 338F/806R primers. The protocols of this analysis were set according to Klindworth (Klindworth et  
253 al., 2013). High-throughput sequencing analysis was conducted using Illumina-MiSeq from Servei de  
254 Genòmica i Bioinformàtica (Barcelona, Spain).

255 The data was manipulated and translated into graphics using RStudio. The taxonomy/abundance heat  
256 tree was created using the Metacoder package (Foster et al., 2017).

257

### 258 **3 Results & Discussion**

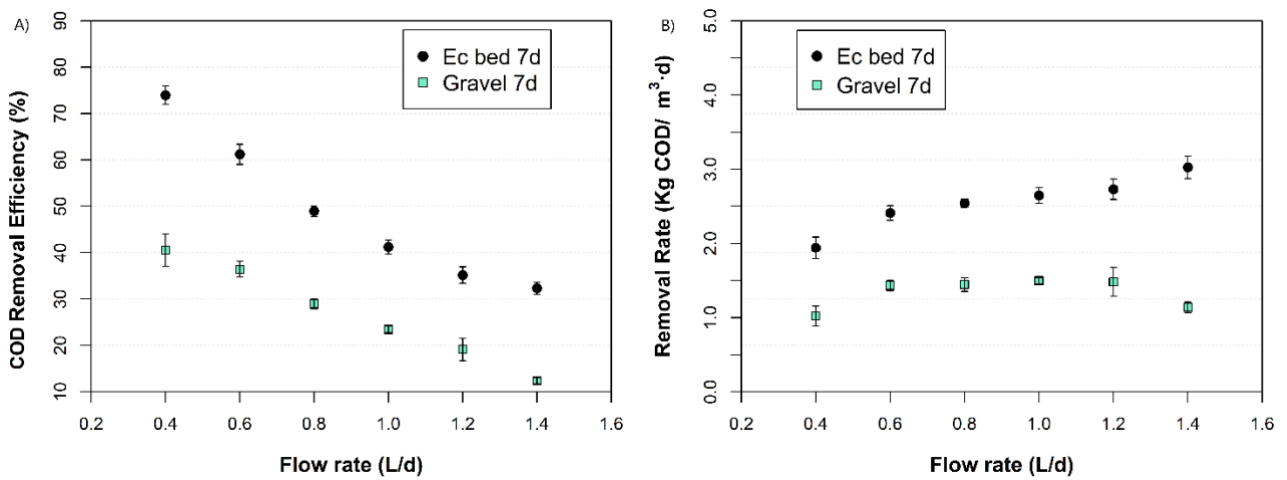
259 The integration of electromicrobiology concepts in treatment wetland gave birth to a new generation  
260 of electroactive biofilters capable electroremediating pollutants from urban wastewater (Mosquera-  
261 Romero et al., 2023). So, providing a strategy for treating industrial wastewater with high organic  
262 load of such pollutants. Thus, the following section includes results revealing how downflow-mode  
263 electroactive biofilters select for a special microbial community capable of removing a mixture of  
264 surfactants from synthetic and real wastewater at low biomass growth yield.

265

266

#### 267 **3.1 Effect of flow rate on electrobioremediation performance under continuous operation**

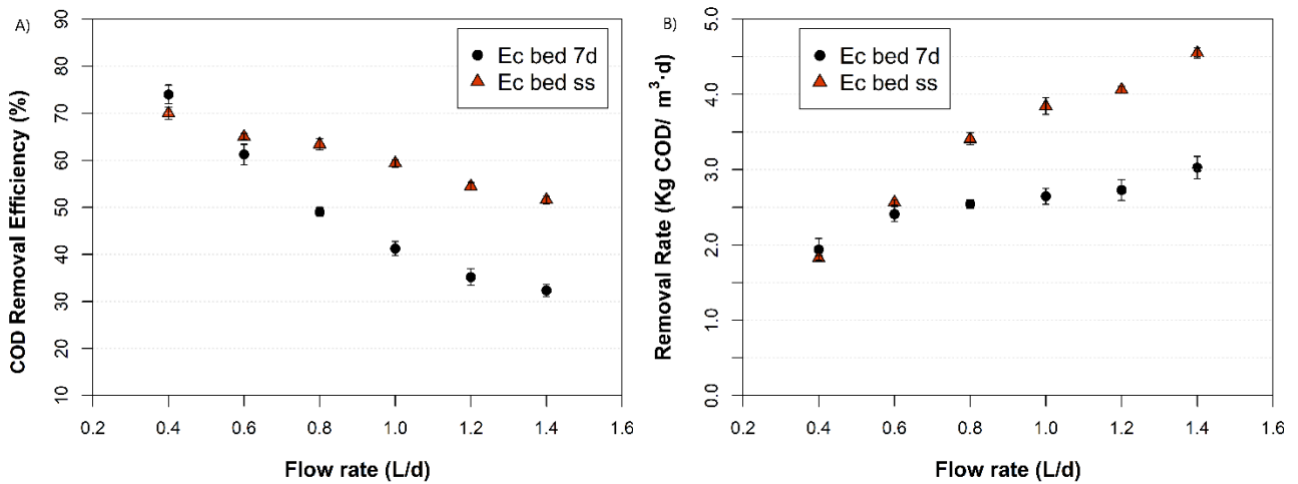
268 The removal efficiency was measured at different flow rates for both reactors, evaluating removal  
269 efficiency and rates per bed volume. At seven days of operation, the biomass generated in each reactor  
270 was assumed to be similar.



271 **Figure 1. Impact of bed material on electrobioremediation performance at different flow rates.** Gravel bed  
272 biofilter at 7 days maturity biofilm (green) and electroconductive bed biofilter at 7 days maturity biofilm (black). a)  
273 Removal Efficiency (%) at different flow rates. b) Removal Rate per unit of bed volume and time at different flow  
274 rates.

275 The removal efficiency decreased as the flow rate increased for the gravel and electroconductive  
276 biofilter under all flow rate conditions. The gravel-based biofilter reached its maximal removal rate at  
277 a flow rate of 0.6 L/h, while the electroactive biofilter increased for all flow rates tested. Indeed, the  
278 gravel biofilter removed a maximum of *ca.* 1.5 kg COD/m<sup>3</sup>·d with no significant variations, while the  
279 electroactive biofilter removed *ca.* 3 kg COD /m<sup>3</sup>·d at its highest rate.

280 The gravel biofilter's operation did not reach a steady state due to the rapid and continuous biomass  
281 accumulation in the gravel biofilter (Figure 2). Nonetheless, steady state operation of the electroactive  
282 biofilter was possible. Therefore, it is possible to compare the impact of a mature biofilm on the  
283 degradation performance.



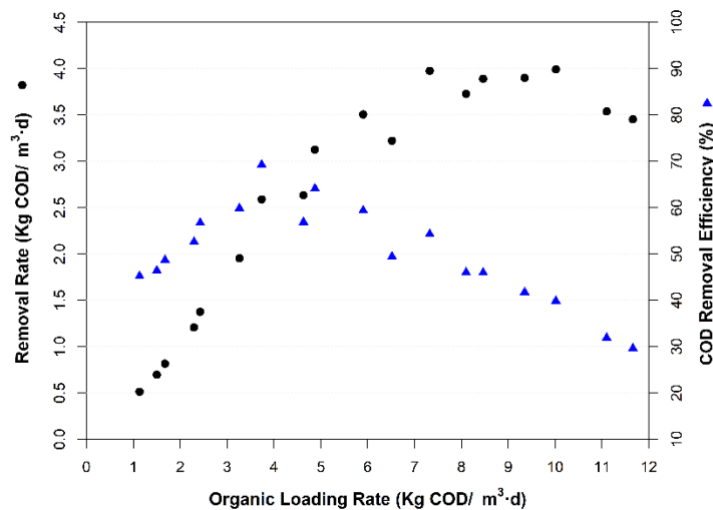
284 **Figure 2. Impact of biomass accumulation on biodegradation performance at different flow rates.**  
 285 Electroactive bed biofilter at steady state (ss) biofilm (red triangles), Electroactive bed biofilter at 7 days maturity  
 286 biofilm (black dots). a) Removal Efficiency (%) at different flow rates. b) Removal Rate as COD kg per cubic  
 287 meter of bed and day at different flow rates.

288 Once the biofilm reaches the state of maturity and stable behavior, the flow rate has a lower impact on  
 289 the removal efficiency, maintaining a higher percentage of removal for the higher flow rates. The  
 290 removal rate increased significantly under steady state reaching 4.5 kg COD/m<sup>3</sup>·d at 1.4 L/d.

291

### 292 3.2 Impact of OLR on electrobioremediation under continuous operation

293 The effect of the organic loading rate (OLR) on the electroactive biofilter was observed by altering the  
 294 concentration of surfactants in the influent while maintaining a steady flow rate of 1 L/d.



295

296 **Figure 3. Organic loading limits the removal efficiency.** Removal rate (left, black circles) and removal efficiency  
 297 (right, blue triangles) for different values of Organic Loading Rate at a fixed flow rate. The electroactive biofilter  
 298 was evaluated with a fixed flow rate of 1L/d.

299

300 The increase of OLR in the electroactive biofilter induced a steady rise in the removal rate up to *ca.* 4  
301 kg COD/m<sup>3</sup>·d. However, an increase in OLR negatively affected removal rates at values higher than  
302 10 kg COD/m<sup>3</sup>·d, where surfactants may have a toxic effect.

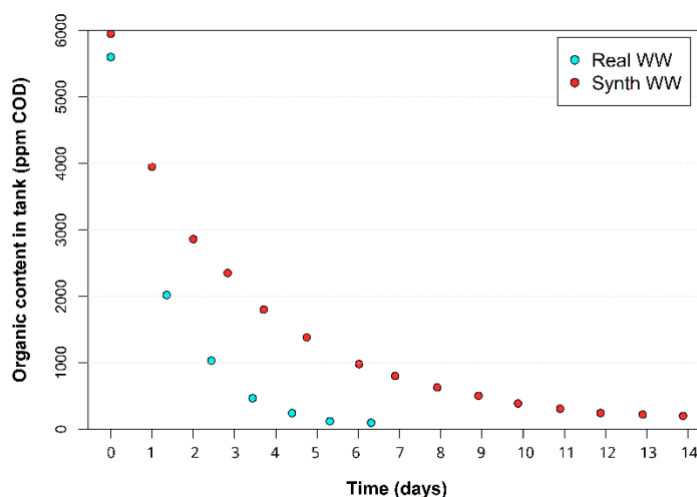
303 At OLR levels below 3 kg COD/m<sup>3</sup>·d, the main limitation seemed to be related to the availability of  
304 organics since both the removal efficiency and rate were relatively low. As the concentration increased,  
305 the removal rate (RR) increased until reaching a plateau. The removal efficiency reached its maximum  
306 between 4-5 kg COD/m<sup>3</sup>·d and then decreased, possibly due to a metabolic respiration bottleneck.

307 Biofilter systems can degrade pollutants at the highest rate near the maximum RR/OLR ratio.  
308 Conventional biofilters are typically used under conditions of low organic loading and relatively high  
309 flow rates and granulometries. Biomass accumulation must be reduced to maintain operability at the  
310 expense of degradation rates. In electroactive biofilters, significantly higher removal rates can be  
311 obtained without detrimental effects on the operation.

312

### 313 3.3 Detergent wastewater biodegradability test

314 An electroactive biofilter was set up to assess the total biodegradability of detergent wastewater in  
315 batch experiments under recirculation mode. Two different detergent mixtures in water were studied,  
316 one synthetic and one from a real surfactant production factory.



317

318 **Figure 4. Biodegradability of surfactant mix in batch.** Evolution of organic content in batch experiments for real  
319 detergent manufacture wastewater and synthetic detergent wastewater in an acclimated lab-scale electroactive  
320 biofilter.

321

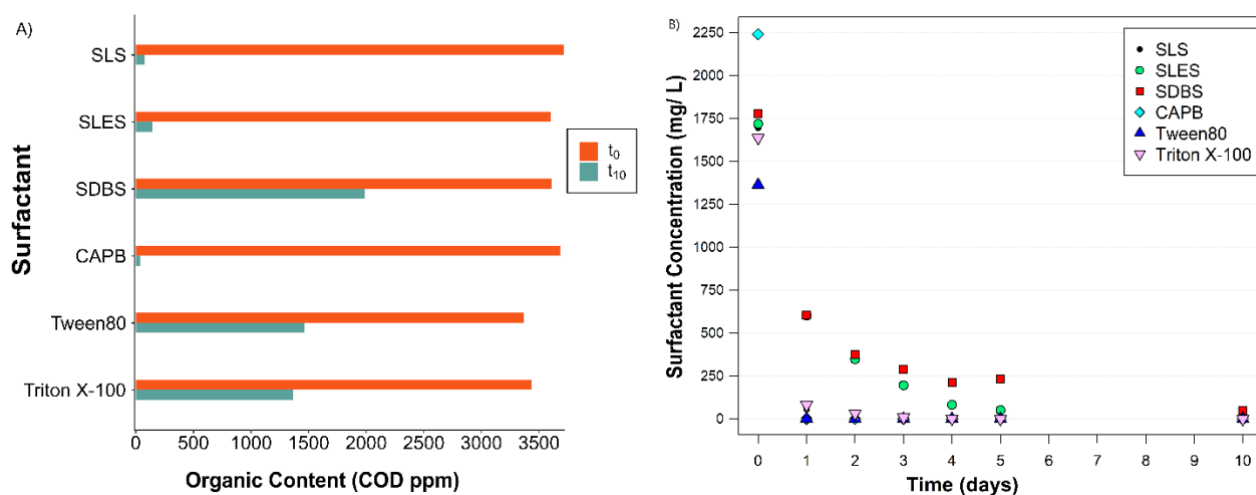
322 In such batch experiments, the reduction in available organic matter causes a reduction in the  
 323 degradation rates, which aligns with previous observations. The real industrial detergent wastewater  
 324 was degraded in 6 days from 5600 to 97 mg/L COD, reaching an asymptotic tendency in the last few  
 325 days (Figure 4). The same phenomenon was observed for the synthetic wastewater at the end of the  
 326 curve, although it took 14 days to achieve COD values as low as 191 mg/L. At the end of each  
 327 experiment, the degradation efficiency was 98.2% for the real water and 96.8% for the synthetic water.

328 Analysis of real wastewater composition revealed the presence of SLS, SLES, SDBS, and CAPB (see  
 329 supplementary section II: table 9). However, after 5 days of recirculation, all pollutants were below  
 330 the detection limit except SDBS (1 ppm). Regarding synthetic wastewater, the surfactants mentioned  
 331 above were removed after 10 days of recirculation, except for SDBS (1.27 ppm).

### 332

### 333 3.4 Degradability of wastewater polluted with single surfactants

334 Batch flasks containing material with 6 individual surfactants were prepared to more precisely test the  
 335 preference for metabolizing and biodegradability of certain surfactants. Initially, inoculum from the  
 336 already active biofilters was supplied to the vessels. Five acclimation runs preceded the measured  
 337 experiments, in which the COD and optical density were monitored (see supplementary section I:  
 338 tables 4 and 5).



339 **Figure 5. Single surfactant biodegradation.** Degradation of independent surfactants in flask vessels containing  
 340 electroconductive material and surfactant solution in a 10-day window, measured by: a) COD content at the beginning  
 341 and the end; b) mg/L of their characteristics' breakdown masses obtained through HPLC-MS.

342

343 All surfactants from our study were analyzed by targeting a characteristic breakdown mass as a proxy  
 344 for the surfactant concentration, except in the case of Tween 80 due to its particular molecular

345 structure. For the linear structured surfactants (SLS, SLES & CAPB), the biodegradation was nearly  
346 complete after 10 days, according to the COD results displayed in Figure 5A (98, 96, and 99 %,  
347 respectively). On the other hand, the surfactants with a more complex molecular structure (SDBS,  
348 Tween 80, and Triton X-100) were partially degraded after 10 days of incubation as determined by  
349 residual COD (45, 57, and 60 %, respectively). However, there was no trace of their characteristic  
350 masses at the end of the treatment (Figure 5B).

351 Indeed, most surfactants quickly degraded despite the high initial concentration. According to the  
352 optical density analysis (supplementary section I: table 4), the highest cell density was reached shortly  
353 after the first 24h in most cases. The highest cell density was observed for the SLS sample, suggesting  
354 the vital role of this surfactant in biological overgrowth. On the other hand, the Tween 80 sample  
355 showed very low cell density compared to the others, slightly more than the media blank. Planktonic  
356 microbial growth was not observed in absence of electroconductive material, suggesting a strong  
357 preference for the microorganisms to grow on the material surface for biodegrading this surfactant.

358 The COD analysis on the abiotic control samples showed decreased concentration in all cases after  
359 including fresh unused granular material (see supplementary section II: table 11). After 4 successive  
360 media renewals (abiotic), the COD values no longer decreased, indicating saturation of the bed  
361 material. An extract of that material showed a Triton X-100 concentration higher than 200 mg/L for  
362 the high-exposure sample and 42 mg/L for the once-exposed sample, confirming that the missing  
363 surfactant was adsorbed.

364 Given the granulometry and specific surface area of materials used in bed biofilters, the adsorption  
365 capacity was expected to be low. In previous works, the porosity and specific surface area were studied,  
366 among other characteristics (Prado et al., 2019), and it was found that the conductive material was in  
367 the same order of magnitude of specific surface area as the gravel ( $<1 \text{ m}^2/\text{gr}$ ). This similarity suggested  
368 a low adsorption capacity, and the rapid saturation of the material confirmed the low relevance of  
369 adsorption phenomena on the removal of surfactant for the medium- and long-term operation of  
370 electroactive biofilters.

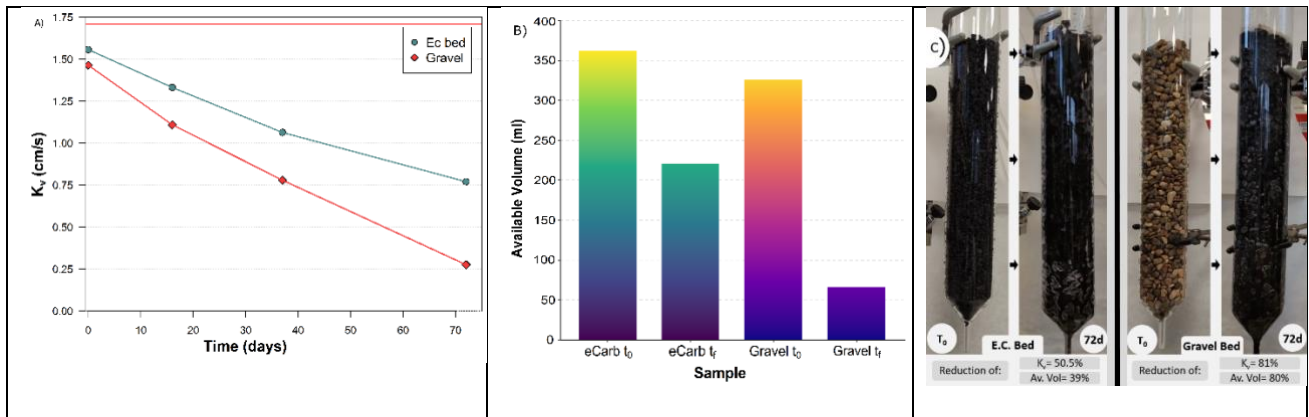
371

### 372 **3.5 Effect of the bed material on the biomass accumulation and hydraulic conductivity**

373 An important aspect to consider in biofilm-based systems is the biomass accumulation's impact on the  
374 hydraulic conductivity. In this regard, bio-clogging is the blockage of pore space due to surplus  
375 microbial biomass accumulation. In biofilters like vertical- flow treatment wetlands, this biomass  
376 accumulation is mainly influenced by OLR, grain size, distribution, and wastewater characteristics

377 (Pucher & Langergraber, 2019). Our experimental conditions were characterized by a relatively high  
378 OLR, a highly biodegradable organic fraction, increased bioavailability of surfactants (Nikpay et al.,  
379 2017), with nutrient availability that, eventually, enabled a fast and continuous biofilm growth over 72  
380 days.

381 To determine the vertical hydraulic conductivity, we applied the gravity drainage method based on  
382 Darcy's law, and the results indicate a different biomass growth rate for each biofilter.



383 **Figure 6. Decrease of hydraulic conductivity and bulk porosity.** Effect of the biomass accumulation on: A) the  
384 hydraulic conductivity at different incubation time; B) the available volume at the beginning and end of the  
385 experiment; C) Image of initial and final state of the electroactive biofilter (left) and gravel biofilter (right).

386

387 The maximum hydraulic conductivity ( $K_v$ ) allowed by the constricted bottom of the glass columns was  
388 1.71 cm/s. The initial values of  $K_v$  for the gravel biofilter and the electroactive biofilter were 1.46 and  
389 1.55 cm/s, respectively. This  $K_v$  was reduced to 0.27 and 0.77 cm/s, respectively, after 72 days of  
390 operation, corresponding to 81.18 % and 50.54 % reductions (Figure 6A). The initially available  
391 volume, considering bulk porosity, was 325ml for the gravel bed, and 362 ml for the electroactive bed,  
392 and eventually it shifted to 66ml and 220 ml after 72 hours, corresponding to a reduction of 79.70 and  
393 39.22 % (Figure 6B).

394 The results showed a higher reduction in hydraulic conductivity in the gravel biofilter despite  
395 removing less COD than the electroactive biofilter ( $5.7 \pm 2.7$  % and  $12.7 \pm 3.2$  %, respectively). An  
396 estimation of biomass growth calculated from the difference in available volume at the beginning and  
397 end of the operation period indicated a reduction of 259 ml for the gravel biofilter and 142 ml for the  
398 electroactive biofilter. This reduction follows the same pattern as the  $K_v$  and the dry biomass tests (see  
399 supplementary section III: tables 18 & 19).

400 These results suggest that biomass accumulation can rapidly render the gravel biofilter inoperative,  
401 leading to impaired performance due to poorer wastewater distribution and oxygen transfer limitation.

402 However, the results of this experiment revealed how a high degradation performance under low  
403 biomass production/accumulation can coexist in electroactive biofilter. Additional studies have  
404 confirmed that electroactive bacteria growing on electrodes result in biofilms of low thickness in  
405 comparison with conventional biofilm growing on inert surfaces, probably due to an intrabiofilm  
406 accumulation of protons that are not consumed during electron electron transfer to electrodes(Pereira  
407 et al., 2023).

408

409

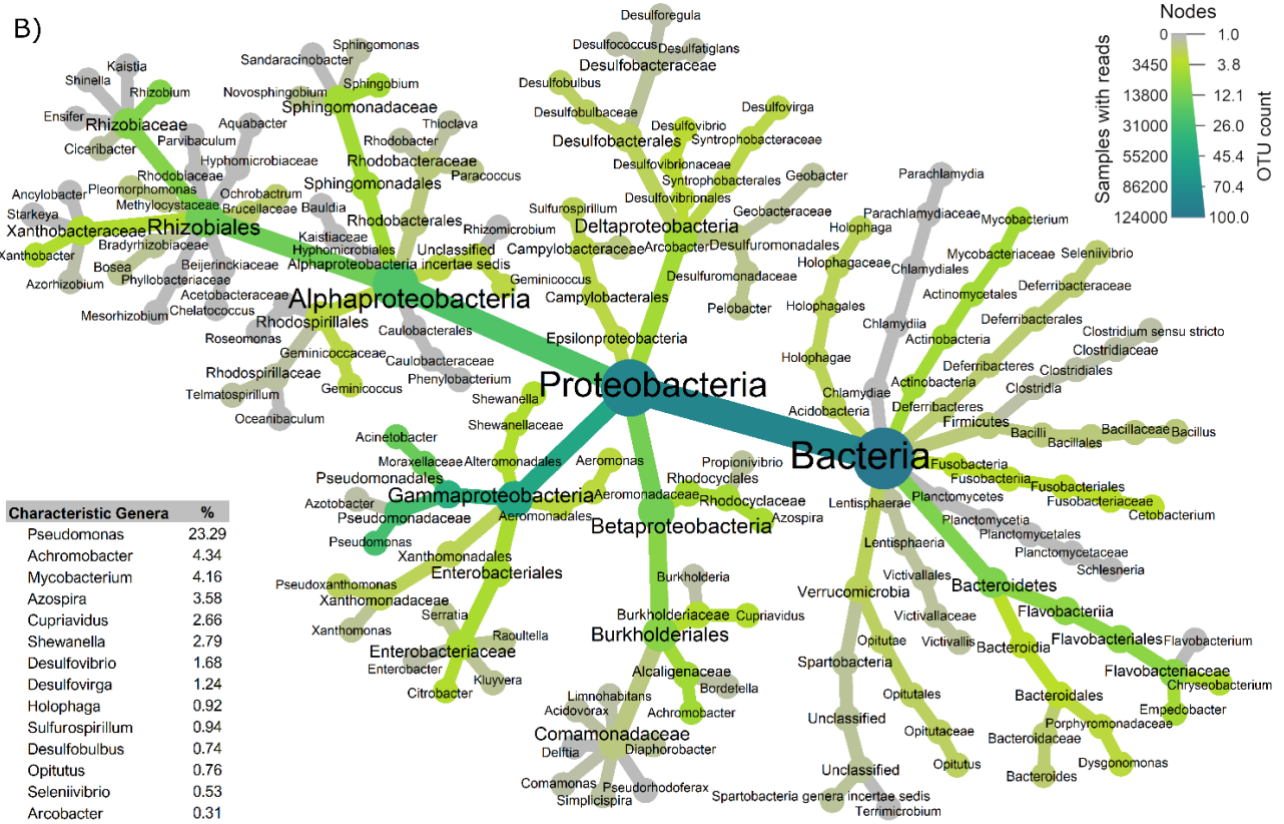
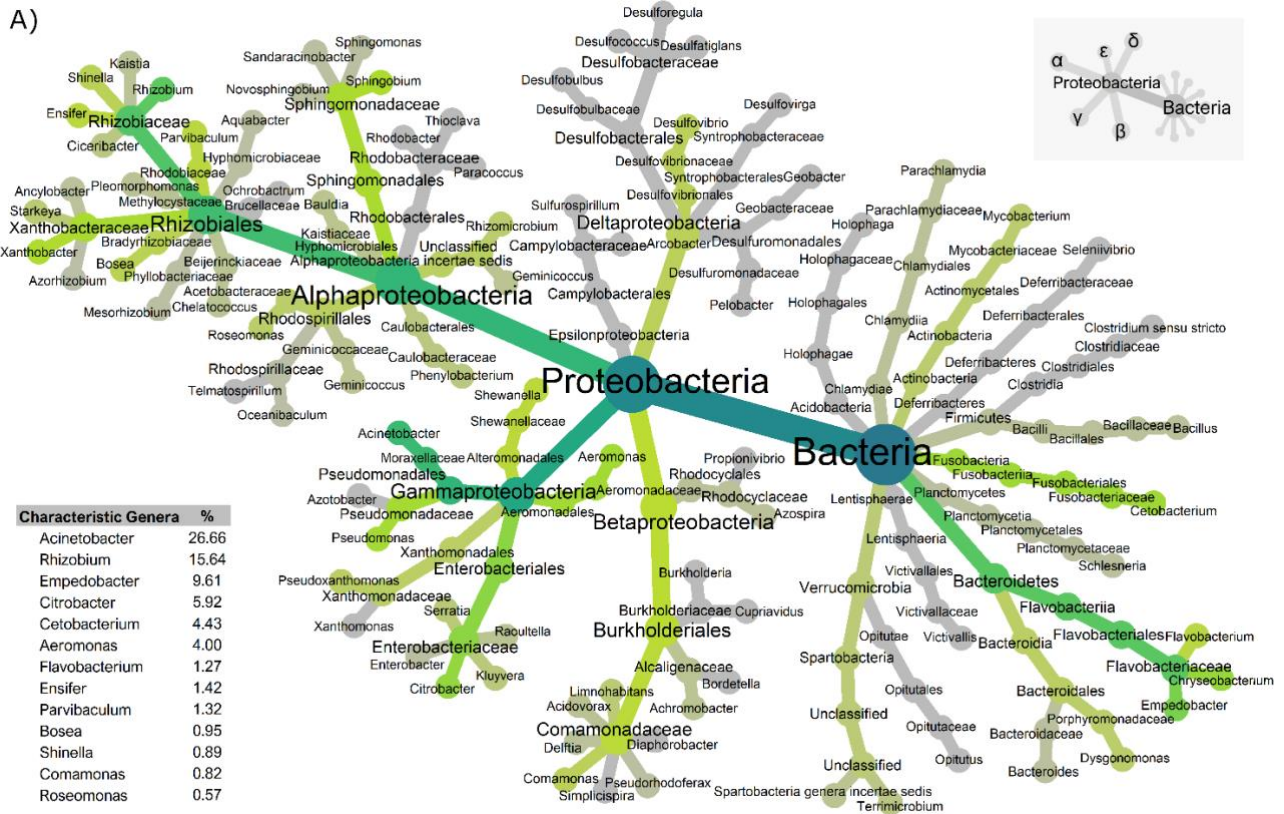
### 410 **3.6 Impact of bed material for selecting microbial communities**

411 All biofilters operated for the microbial community analysis shared the same operating conditions,  
412 reactor size, shape, material granulometry, and inoculum. Therefore, the only factors affecting  
413 microbial community can be attributed to the bed material's composition and properties.

414 Duplicate particles were selected from both reactors for microbial community analysis through 16S  
415 sequencing, and significant differences were found between the gravel and electroactive biofilter  
416 communities. The taxonomic information and normalized relative abundance were graphically  
417 displayed as heat trees.

418





419 **Figure 7. Microbial Heat Tree.** Graphical representation of microbial populations by taxonomy and relative  
 420 abundance: a) M. population developed over gravel granules; b) M. population developed over electroconductive  
 421 carbon granules.

422 As an estimation of the alpha diversity, the Shannon index for the electroconductive material samples  
423 was 2.99, and for the gravel granules biofilm 2.73. Regarding beta diversity, the Bray-Curtis index  
424 between both communities is  $0.52\pm 0.04$ , which indicates a relatively high difference between the  
425 communities.

426 There were common occurrences of many Genera when comparing the microbial populations  
427 established in both bed materials. All these common genera were previously classified as aerobes or  
428 facultative anaerobes except for *Cetobacterium*, which is micro-aerotolerant. Selecting the most  
429 representative differential genera for each population (see supplementary section IV, figure 5), all but  
430 one in the gravel population were aerobic. In contrast, the microbial community colonizing the  
431 electroconductive bed was all anaerobic or facultatively anaerobic. A similar pattern was observed in  
432 the global populations (evaluating 96% of the population). For the gravel population, only 1% were  
433 anaerobic, 4.4% were micro-aerotolerant, 26.7% facultative anaerobes, and 63.5% were aerobic  
434 microorganisms. For the electroconductive bed population, 10.5% were anaerobic, 2.3% were micro-  
435 aerotolerant, 48.6% were facultative anaerobes, and 34.6% were aerobic microorganisms (see  
436 supplementary section IV, figure 6).

437 Some of the major genera such as *Pseudomonas* (Chen et al., 2019; Jovicic et al., 2010; Paulo et al.,  
438 2017), *Rhizobium* (Merkova et al., 2018), *Acinetobacter* (Hosseini et al., 2007), *Citrobacter* (Dhouib  
439 et al., 2003), *Aeromonas* (Paulo et al., 2017), *Comamonas* (Paulo et al., 2017), present in both systems  
440 were previously reported to participate in surfactant biodegradation. These genera suggest a primary  
441 degradation role of the aerobic and the facultative anaerobes dominating the outer layers of the biofilm.

442 Looking deeper into the anaerobes and facultative anaerobes of the electroconductive carbon biofilter's  
443 population, electroactive microorganisms represented 10.8% of the global population including  
444 *Shewanella Xiamenensis* (Truong et al., 2021), *Cupriavidus Metallidurans* (Alviz-gazitua et al., 2022),  
445 *Arcobacter Butzleri* (Fedorovich et al., 2009), *Bacillus Cereus* (Islam et al., 2017), *Citrobacter*  
446 *Freundii*, *Desulfovibrio Desulfuricans*, *Geobacter Lovlyi* and *Geothrix Fermentans* (Koch & Harnisch,  
447 2016). There are additional members that are frequently found in electroactive biofilms or belonging  
448 to genera with electroactive members, adding up to an additional 31%.

449 Bacteria from *Pseudomonas* genus is known for their metabolic versatility (aerobic and anaerobic) and  
450 their capacity for surfactant degradation, with some producing electron shuttles (Rabaey et al., 2005).  
451 At the genus level, *Pseudomonas* represented 4.1% of the gravel population, whereas, in the  
452 electroconductive bed population, they represented up to 21.9%. Surprisingly, a single unclassified  
453 species dominated the latter, accounting for 19% of the community. This population can be vital for

454 protecting the anaerobic layers of the biofilm since some bacteria from *Pseudomonas* genus have been  
455 previously reported to thrive in microaerophilic conditions and to deplete O<sub>2</sub> at the interior portions of  
456 biofilms (Alvarez-Ortega & Harwood, 2007).

457 The presence of surfactants in the studied systems could facilitate electron transfer mechanisms, given  
458 that the cellular membrane permeability is modified by surfactants (Sotirova et al., 2008). Previous  
459 studies on microbial electrochemistry have shown an increase in the electrical current generation or  
460 power generation after adding small doses of surfactants (Oluwaseun, 2015; Ren et al., 2012; Song et  
461 al., 2015), and vast reductions in the internal resistance (Pasternak et al., 2020). Furthermore,  
462 molecules such as phenazine-1-carboxamide (PCN), known electron shuttles (Rabaey et al., 2005),  
463 combined with surfactants were able to boost the current generation of a gram-positive bacteria (Pham  
464 et al., 2008).

465

### 466 **3.7 Bioelectrochemistry as a booster for conventional downflow (aerobic) biofilters to treat** 467 **wastewater**

468 The role played by electroactive microorganisms in the performance of flooded METland<sup>®</sup> systems  
469 has already been demonstrated (Peñacoba-Antona et al., 2022b; Prado et al., 2020) to overcome  
470 microbial electron acceptor limitation typically present when anoxia meets any inert material bed.  
471 Indeed, the use of aeration was excluded from microbial electrochemistry in routinary basis, under the  
472 assumption that oxygen inhibits electroactive bacteria by competing with electrode for harvesting  
473 electrons from microbial metabolism. However, and according to the microbial community analysis,  
474 the electroconductive material supports the formation an anaerobic community capable of respiring  
475 the electroconductive bed, together with aerobic and facultative anaerobic microorganisms capable of  
476 using O<sub>2</sub>, presumably, in the outer layers of the same biofilm. Actually, the presence of bacteria from  
477 *Geobacter* genus was previously reported in down-flow electroactive biofilter where oxygen was  
478 available (Aguirre et al., 2020). In this context, such complex electroactive metabolic pipeline helps  
479 regulate biomass formation and boost microbial metabolism.

480 This phenomenon could only be attributed to the properties of electroactive microbial communities  
481 forming the biofilm. An important contributing factor to this limited growth could be the biofilm's  
482 acidification due to proton accumulation as a consequence of the charge unbalances during electrode  
483 respiration (Franks et al., 2009). More recently, energetic considerations in the electron transfer  
484 mechanisms have been pointed out as growth regulating mechanisms, increasing product/biomass  
485 yields in the presence of electroactive microorganisms (Moscoviz et al., 2017). This phenomenon was

486 confirmed and expanded with the demonstration of a hybrid metabolism (fermentation-respiration)  
487 that, through the use of extracellular electron transfer, alters the NAD<sup>+</sup>/NADH ratios, increases  
488 product/biomass yields, and increases cellular metabolic fluxes (Tejedor-Sanz et al., 2022).

489 The high treatment performance of electroactive biofilters, together with the long-term operation with  
490 limited biomass accumulation, suggest the feasibility of the technology for the treatment of wastewater  
491 polluted with surfactant content. According to the results, achieving sewer discharge limits for urban  
492 or industrial wastewater effluents is feasible.

493 The microbial resilience provided by the sheltering properties of the biofilm and of the biofilter bed  
494 material enables the survival of microbial communities despite the presence of pollutants in  
495 concentrations that are toxic under planktonic communities. Additionally, these properties allow a  
496 more diverse microbial community, including electroactive bacteria, in this manner, increasing the  
497 metabolic toolkit.

498 Finally, the results obtained in this study let us to conclude that passive-aerated electroactive biofilters  
499 are sustainable and efficient solution for biodegrading detergents at low energy cost and no sludge  
500 production, so we can anticipate their application to the treatment of laundry wastewater, car wash  
501 effluents, or similar waste, especially in remote sites with no access to sewer systems.

502

503

504

505

#### 506 **Credit authorship contribution statement**

507 **Eduardo Noriega:** Conceptualization, Methodology, Investigation, Formal analysis, Visualization,  
508 Writing – original draft. **María Isabel López:** Analytical supervision, Formal analysis. **Abraham**  
509 **Esteve-Núñez:** Conceptualization, Writing – review & editing, Supervision.

510

#### 511 **Declaration of Competing Interest**

512 The authors declare that there are no conflicts of interest to the best of their knowledge that could  
513 influence the work reported in this article.

514

515 **Acknowledgments**

516 This work has been made possible by the Spanish Ministry of Science, Innovation and Universities  
517 (Grant Ref: DIN2018-009782) and the University of Alcalá (UAH) through the support of the  
518 Industrial PhD fellowship of Eduardo Noriega Primo. This research was co-financed by Metfilter S.L.

519

520 **References**

- 521 Aguirre-Sierra, A., Bacchetti-De Gregoris, T., Berná, A., Salas, J. J., Aragón, C., & Esteve-Núñez, A. (2016).  
522 Microbial electrochemical systems outperform fixed-bed biofilters in cleaning up urban wastewater.  
523 *Environmental Science: Water Research and Technology*, 2(6), 984–993.  
524 <https://doi.org/10.1039/c6ew00172f>
- 525 Aloui, F., Kchaou, S., & Sayadi, S. (2009). Physicochemical treatments of anionic surfactants wastewater:  
526 Effect on aerobic biodegradability. *Journal of Hazardous Materials*, 164(1), 353–359.  
527 <https://doi.org/10.1016/j.jhazmat.2008.08.009>
- 528 Alvarez-Ortega, C., & Harwood, C. S. (2007). Responses of *Pseudomonas aeruginosa* to low oxygen indicate  
529 that growth in the cystic fibrosis lung is by aerobic respiration. *Molecular Microbiology*, 65(1), 153–165.  
530 <https://doi.org/10.1111/j.1365-2958.2007.05772.x>
- 531 Alviz-gazitua, P., Espinoza-tofalos, A., Formicola, F., Guiliani, N., Turner, R. J., Franzetti, A., & Seeger, M.  
532 (2022). Enhanced Exoelectrogenic Activity of *Cupriavidus metallidurans* in Bioelectrochemical Systems  
533 through the Expression of a Constitutively Active Diguanilate Cyclase.
- 534 Arora, J., Ranjan, A., Chauhan, A., Biswas, R., Rajput, V. D., Sushkova, S., Mandzhieva, S., Minkina, T., &  
535 Jindal, T. (2022). Surfactant pollution, an emerging threat to ecosystem: Approaches for effective  
536 bacterial degradation. *Journal of Applied Microbiology*, 133(3), 1229–1244.  
537 <https://doi.org/10.1111/jam.15631>
- 538 Berna, J. L., Ferrer, J., Moreno, A., Prats, D., & Ruiz Bevia, F. (1991). The Behaviour of LAS in the  
539 environment. *Journal of Chemical Technology and Biotechnology*, 50, 387–398.  
540 <https://doi.org/10.1002/jctb.280500310>
- 541 Bond, D. R., & Lovley, D. R. (2003). Electricity Production by *Geobacter sulfurreducens* Attached to  
542 Electrodes. *Applied and Environmental Microbiology*, 69(3), 1548–1555.  
543 <https://doi.org/10.1128/AEM.69.3.1548-1555.2003>
- 544 Camacho-Muñoz, D., Martín, J., Santos, J. L., Aparicio, I., & Alonso, E. (2014). Occurrence of surfactants in  
545 wastewater: Hourly and seasonal variations in urban and industrial wastewaters from Seville (Southern  
546 Spain). *Science of the Total Environment*, 468–469, 977–984.  
547 <https://doi.org/10.1016/j.scitotenv.2013.09.020>
- 548 Chen, Y., Wang, C., Dong, S., Jiang, L., Shi, Y., Li, X., Zou, W., & Tan, Z. (2019). Microbial community  
549 assembly in detergent wastewater treatment bioreactors: Influent rather than inoculum source plays a  
550 more important role. *Bioresource Technology*, 287(March), 121467.  
551 <https://doi.org/10.1016/j.biortech.2019.121467>
- 552 Dhouib, A., Hamad, N., Hassaïri, I., & Sayadi, S. (2003). Degradation of anionic surfactants by *Citrobacter*  
553 *braakii*. *Process Biochemistry*, 38(8), 1245–1250. [https://doi.org/10.1016/S0032-9592\(02\)00322-9](https://doi.org/10.1016/S0032-9592(02)00322-9)

- 554 Fedorovich, V., Knighton, M. C., Pagaling, E., Ward, F. B., Free, A., & Goryanin, I. (2009). Novel  
555 electrochemically active bacterium phylogenetically related to *Arcobacter butzleri*, isolated from a  
556 microbial fuel cell. *Applied and Environmental Microbiology*, *75*(23), 7326–7334.  
557 <https://doi.org/10.1128/AEM.01345-09>
- 558 Fogler, H. S. (2006). *Elements of Chemical Reaction Engineering* (4th Ed.). Prentice Hall PTR.
- 559 Foster, Z. S. L., Sharpton, T. J., & Grünwald, N. J. (2017). Metacoder: An R package for visualization and  
560 manipulation of community taxonomic diversity data. *PLoS Computational Biology*, *13*(2), 1–15.  
561 <https://doi.org/10.1371/journal.pcbi.1005404>
- 562 Franks, A. E., Nevin, K. P., Jia, H., Izallalen, M., Woodard, T. L., & Lovley, D. R. (2009). Novel strategy for  
563 three-dimensional real-time imaging of microbial fuel cell communities: Monitoring the inhibitory  
564 effects of proton accumulation within the anode biofilm. *Energy and Environmental Science*, *2*(1), 113–  
565 119. <https://doi.org/10.1039/b816445b>
- 566 Gefell, M. J., Larue, M., & Russell, K. (2019). Vertical Hydraulic Conductivity Measurement by Gravity  
567 Drainage. *Groundwater*, *57*(4), 511–516. <https://doi.org/10.1111/gwat.12911>
- 568 Hosseini, F., Malekzadeh, F., Amirmozafari, N., & Ghaemi, N. (2007). Biodegradation of anionic surfactants  
569 by isolated bacteria from activated sludge. *International Journal of Environmental Science and*  
570 *Technology*, *4*(1), 127–132. <https://doi.org/10.1007/BF03325970>
- 571 Hwang, J. H., Kim, K. Y., Resurreccion, E. P., & Lee, W. H. (2019). Surfactant addition to enhance  
572 bioavailability of bilge water in single chamber microbial fuel cells (MFCs). *Journal of Hazardous*  
573 *Materials*, *368*(February), 732–738. <https://doi.org/10.1016/j.jhazmat.2019.02.007>
- 574 Islam, M. A., Ethiraj, B., Cheng, C. K., Yousuf, A., & Khan, M. M. R. (2017). Electrogenic and  
575 Antimethanogenic Properties of *Bacillus cereus* for Enhanced Power Generation in Anaerobic Sludge-  
576 Driven Microbial Fuel Cells. *Energy and Fuels*, *31*(6), 6132–6139.  
577 <https://doi.org/10.1021/acs.energyfuels.7b00434>
- 578 Ivanković, T., & Hrenović, J. (2010). Surfactants in the environment. *Arhiv Za Higijenu Rada i Toksikologiju*,  
579 *61*(1), 95–110. <https://doi.org/10.2478/10004-1254-61-2010-1943>
- 580 Jensen, J. (1999). Fate and effects of linear alkylbenzene sulphonates (LAS) in the terrestrial environment.  
581 *Science of the Total Environment*, *226*(2–3), 93–111. [https://doi.org/10.1016/S0048-9697\(98\)00395-7](https://doi.org/10.1016/S0048-9697(98)00395-7)
- 582 Jovicic, B., Venturi, V., Davison, J., Topisirovic, L., & Kojic, M. (2010). Regulation of the sdsA alkyl  
583 sulfatase of *Pseudomonas* sp. ATCC19151 and its involvement in degradation of anionic surfactants.  
584 *Journal of Applied Microbiology*, *109*(3), 1076–1083. <https://doi.org/10.1111/j.1365-2672.2010.04738.x>
- 585 Justin, M. Z., Vrhovšek, D., Stuhlbacher, A., & Bulc, T. G. (2009). Treatment of wastewater in hybrid  
586 constructed wetland from the production of vinegar and packaging of detergents. *Desalination*, *246*(1–  
587 3), 100–109. <https://doi.org/10.1016/j.desal.2008.03.045>
- 588 Kim, D., Kim, J., Lee, K. W., & Lee, T. S. (2019). Removal of sodium dodecylbenzenesulfonate using  
589 surface-functionalized mesoporous silica nanoparticles. *Microporous and Mesoporous Materials*,  
590 *275*(September 2018), 270–277. <https://doi.org/10.1016/j.micromeso.2018.09.007>
- 591 Klindworth, A., Pruesse, E., Schweer, T., Peplies, J., Quast, C., Horn, M., & Glöckner, F. O. (2013).  
592 Evaluation of general 16S ribosomal RNA gene PCR primers for classical and next-generation  
593 sequencing-based diversity studies. *Nucleic Acids Research*, *41*(1), 1–11.  
594 <https://doi.org/10.1093/nar/gks808>

- 595 Koch, C., & Harnisch, F. (2016). Is there a Specific Ecological Niche for Electroactive Microorganisms?  
596 *ChemElectroChem*, 3(9), 1282–1295. <https://doi.org/10.1002/celec.201600079>
- 597 Liwarska-Bizukoja, E., Miksch, K., Malachowska-Jutysz, A., & Kalka, J. (2005). Acute toxicity and  
598 genotoxicity of five selected anionic and nonionic surfactants. *Chemosphere*, 58(9), 1249–1253.  
599 <https://doi.org/10.1016/j.chemosphere.2004.10.031>
- 600 Merkova, M., Zalesak, M., Ringlova, E., Julinova, M., & Ruzicka, J. (2018). Degradation of the surfactant  
601 Cocamidopropyl betaine by two bacterial strains isolated from activated sludge. *International*  
602 *Biodeterioration and Biodegradation*, 127(December 2017), 236–240.  
603 <https://doi.org/10.1016/j.ibiod.2017.12.006>
- 604 Merrettig-Bruns, U., & Jelen, E. (2009). Anaerobic biodegradation of detergent surfactants. *Materials*, 2(1),  
605 181–206. <https://doi.org/10.3390/ma2010181>
- 606 Moscoviz, R., Flayac, C., Desmond-Le Quémener, E., Trably, E., & Bernet, N. (2017). Revealing  
607 extracellular electron transfer mediated parasitism: energetic considerations. *Scientific Reports*, 7(1), 1–  
608 9. <https://doi.org/10.1038/s41598-017-07593-y>
- 609 Mosquera-Romero, S., Ntagia, E., Rousseau, D. P. L., Esteve-Núñez, A., & PrévotEAU, A. (2023). Water  
610 treatment and reclamation by implementing electrochemical systems with constructed wetlands.  
611 *Environmental Science and Ecotechnology*, 16. <https://doi.org/10.1016/j.ese.2023.100265>
- 612 Nikpay, M., Krebs, P., & Ellis, B. (2017). A Review of Surfactant Role in Soil Clogging Processes at  
613 Wastewater Exfiltration Locations in Sewers. *Water Environment Research*, 89(8), 714–723.  
614 <https://doi.org/10.2175/106143017x14902968254647>
- 615 Oluwaseun, A. (2015). Bioremediation of Petroleum Hydrocarbons using Microbial Fuel Cells. *PhD Thesis by*  
616 *the University of Westminster*.
- 617 Panizza, M., Delucchi, M., & Cerisola, G. (2005). Electrochemical degradation of anionic surfactants. *Journal*  
618 *of Applied Electrochemistry*, 35(4), 357–361. <https://doi.org/10.1007/s10800-005-0793-x>
- 619 Pasternak, G., Askitosari, T. D., & Rosenbaum, M. A. (2020). Biosurfactants and Synthetic Surfactants in  
620 Bioelectrochemical Systems: A Mini-Review. *Frontiers in Microbiology*, 11(March), 1–9.  
621 <https://doi.org/10.3389/fmicb.2020.00358>
- 622 Paulo, A. M. S., Aydin, R., Dimitrov, M. R., Vreeling, H., Cavaleiro, A. J., García-Encina, P. A., Stams, A. J.  
623 M., & Plugge, C. M. (2017). Sodium lauryl ether sulfate (SLES) degradation by nitrate-reducing  
624 bacteria. *Applied Microbiology and Biotechnology*, 101(12), 5163–5173. <https://doi.org/10.1007/s00253-017-8212-x>
- 626 Peñacoba-Antona, L., Ramirez-Vargas, C. A., Wardman, C., Carmona-Martinez, A. A., Esteve-Núñez, A.,  
627 Paredes, D., Brix, H., & Arias, C. A. (2022a). Microbial Electrochemically Assisted Treatment  
628 Wetlands: Current Flow Density as a Performance Indicator in Real-Scale Systems in Mediterranean and  
629 Northern European Locations. *Frontiers in Microbiology*, 13(April).  
630 <https://doi.org/10.3389/fmicb.2022.843135>
- 631 Peñacoba-Antona, L., Ramirez-Vargas, C. A., Wardman, C., Carmona-Martinez, A. A., Esteve-Núñez, A.,  
632 Paredes, D., Brix, H., & Arias, C. A. (2022b). Microbial Electrochemically Assisted Treatment  
633 Wetlands: Current Flow Density as a Performance Indicator in Real-Scale Systems in Mediterranean and  
634 Northern European Locations. *Frontiers in Microbiology*, 13(April).  
635 <https://doi.org/10.3389/fmicb.2022.843135>



- 636 Pereira, J., Neves, P., Nemanic, V., Pereira, M. A., Sleutels, T., Hamelers, B., & Heijne, A. ter. (2023).  
637 Starvation combined with constant anode potential triggers intracellular electron storage in electro-active  
638 biofilms. *Water Research*, 242. <https://doi.org/10.1016/j.watres.2023.120278>
- 639 Pham, T. H., Boon, N., Aelterman, P., Clauwaert, P., De Schamphelaire, L., Vanhaecke, L., De Maeyer, K.,  
640 Höfte, M., Verstraete, W., & Rabaey, K. (2008). Metabolites produced by *Pseudomonas* sp. enable a  
641 Gram-positive bacterium to achieve extracellular electron transfer. *Applied Microbiology and*  
642 *Biotechnology*, 77(5), 1119–1129. <https://doi.org/10.1007/s00253-007-1248-6>
- 643 Prado, A., Berenguer, R., & Esteve-Núñez, A. (2019). Electroactive biochar outperforms highly conductive  
644 carbon materials for biodegrading pollutants by enhancing microbial extracellular electron transfer.  
645 *Carbon*, 146, 597–609. <https://doi.org/10.1016/j.carbon.2019.02.038>
- 646 Prado, A., Berenguer, R., & Esteve-Núñez, A. (2022). Evaluating bioelectrochemically-assisted constructed  
647 wetland (METland®) for treating wastewater: Analysis of materials, performance and electroactive  
648 communities. *Chemical Engineering Journal*, 440(February), 135748.  
649 <https://doi.org/10.1016/j.cej.2022.135748>
- 650 Prado, A., Ramírez-Vargas, C. A., Arias, C. A., & Esteve-Núñez, A. (2020). Novel bioelectrochemical  
651 strategies for domesticating the electron flow in constructed wetlands. *Science of the Total Environment*,  
652 735, 139522. <https://doi.org/10.1016/j.scitotenv.2020.139522>
- 653 Pucher, B., & Langergraber, G. (2019). The state of the art of clogging in vertical flow Wetlands. *Water*  
654 *(Switzerland)*, 11(11). <https://doi.org/10.3390/w11112400>
- 655 Rabaey, K., Boon, N., Höfte, M., & Verstraete, W. (2005). Microbial phenazine production enhances electron  
656 transfer in biofuel cells. *Environmental Science and Technology*, 39(9), 3401–3408.  
657 <https://doi.org/10.1021/es048563o>
- 658 Radeef, A. Y., & Ismail, Z. Z. (2021). Bioelectrochemical treatment of actual carwash wastewater associated  
659 with sustainable energy generation in three-dimensional microbial fuel cell. *Bioelectrochemistry*, 142,  
660 107925. <https://doi.org/10.1016/j.bioelechem.2021.107925>
- 661 Ramírez-Vargas, C. A., Arias, C. A., Carvalho, P., Zhang, L., Esteve-Núñez, A., & Brix, H. (2019).  
662 Electroactive biofilm-based constructed wetland (EABB-CW): A mesocosm-scale test of an innovative  
663 setup for wastewater treatment. *Science of The Total Environment*, 659, 796–806.  
664 <https://doi.org/10.1016/j.scitotenv.2018.12.432>
- 665 Ren, L., Tokash, J. C., Regan, J. M., & Logan, B. E. (2012). Current generation in microbial electrolysis cells  
666 with addition of amorphous ferric hydroxide, Tween 80, or DNA. *International Journal of Hydrogen*  
667 *Energy*, 37(22), 16943–16950. <https://doi.org/10.1016/j.ijhydene.2012.08.119>
- 668 Sarkar, R., Pal, A., Rakshit, A., & Saha, B. (2021). Properties and applications of amphoteric surfactant: A  
669 concise review. *Journal of Surfactants and Detergents*, 24(5), 709–730.  
670 <https://doi.org/10.1002/jsde.12542>
- 671 Schinkel, L., Lara-Martín, P. A., Giger, W., Hollender, J., & Berg, M. (2022). Synthetic surfactants in Swiss  
672 sewage sludges: Analytical challenges, concentrations and per capita loads. *Science of the Total*  
673 *Environment*, 808, 151361. <https://doi.org/10.1016/j.scitotenv.2021.151361>
- 674 Scott, M. J., & Jones, M. N. (2000). The biodegradation of surfactants in the environment. *Biochimica et*  
675 *Biophysica Acta - Biomembranes*, 1508(1–2), 235–251. [https://doi.org/10.1016/S0304-4157\(00\)00013-7](https://doi.org/10.1016/S0304-4157(00)00013-7)
- 676 Šíma, J., & Holcová, V. (2011). Removal of nonionic surfactants from wastewater using a constructed  
677 wetland. *Chemistry and Biodiversity*, 8(10), 1819–1832. <https://doi.org/10.1002/cbdv.201100063>



- 678 Song, Y.-C., Kim, D.-S., Woo, J.-H., Subha, B., Jang, S.-H., & Sivakumar, S. (2015). Effect of surface  
679 modification of anode with surfactant on the performance of microbial fuel cell. *International Journal of*  
680 *Energy Research*, 39(6), 860–868. <https://doi.org/10.1002/er.3284>
- 681 Sotirova, A. V., Spasova, D. I., Galabova, D. N., Karpenko, E., & Shulga, A. (2008). Rhamnolipid-  
682 biosurfactant permeabilizing effects on gram-positive and gram-negative bacterial strains. *Current*  
683 *Microbiology*, 56(6), 639–644. <https://doi.org/10.1007/s00284-008-9139-3>
- 684 Tejedor-Sanz, S., Stevens, E. T., Li, S., Finnegan, P., Nelson, J., Knoesen, A., Light, S. H., Ajo-Franklin, C.  
685 M., & Marco, M. L. (2022). Extracellular electron transfer increases fermentation in lactic acid bacteria  
686 via a hybrid metabolism. *ELife*, 11, 1–29. <https://doi.org/10.7554/ELIFE.70684>
- 687 Truong, D. H., Dam, M. S., Bujna, E., Rezessy-Szabo, J., Farkas, C., Vi, V. N. H., Csernus, O., Nguyen, V.  
688 D., Gathergood, N., Friedrich, L., Hafidi, M., Gupta, V. K., & Nguyen, Q. D. (2021). In situ fabrication  
689 of electrically conducting bacterial cellulose-polyaniline-titanium-dioxide composites with the  
690 immobilization of *Shewanella xiamenensis* and its application as bioanode in microbial fuel cell. *Fuel*,  
691 285(May 2020). <https://doi.org/10.1016/j.fuel.2020.119259>
- 692 Wang, X., Aulenta, F., Puig, S., Esteve-Núñez, A., He, Y., Mu, Y., & Rabaey, K. (2020). Microbial  
693 electrochemistry for bioremediation. *Environmental Science and Ecotechnology*, 1, 100013.  
694 <https://doi.org/10.1016/j.ese.2020.100013>
- 695 Wang, X. J., Song, Y., & Mai, J. S. (2008). Combined Fenton oxidation and aerobic biological processes for  
696 treating a surfactant wastewater containing abundant sulfate. *Journal of Hazardous Materials*, 160(2–3),  
697 344–348. <https://doi.org/10.1016/j.jhazmat.2008.02.117>
- 698 Yang, S., Du, F., & Liu, H. (2012). Characterization of mixed-culture biofilms established in microbial fuel  
699 cells. *Biomass and Bioenergy*, 46, 531–537. <https://doi.org/10.1016/j.biombioe.2012.07.007>
- 700 Ying, G. G. (2006). Fate, behavior and effects of surfactants and their degradation products in the  
701 environment. *Environment International*, 32(3), 417–431. <https://doi.org/10.1016/j.envint.2005.07.004>
- 702 Zhang, Y., Jiang, J., Zhao, Q., Gao, Y. Z., Wang, K., Ding, J., Yu, H., & Yao, Y. (2017). Accelerating anodic  
703 biofilms formation and electron transfer in microbial fuel cells: Role of anionic biosurfactants and  
704 mechanism. *Bioelectrochemistry*, 117, 48–56. <https://doi.org/10.1016/j.bioelechem.2017.06.002>
- 705